

Finite conductivity in mesoscopic Hall bars of inverted InAs/GaSb quantum wells

Ivan Knez* and R. R. Du

Department of Physics and Astronomy, Rice University, Houston, Texas 77251-1892, USA

Gerard Sullivan

Teledyne Scientific and Imaging, Thousand Oaks, California, 91360, USA

(Received 27 January 2010; revised manuscript received 14 April 2010; published 4 May 2010)

We have studied experimentally the low-temperature conductivity of mesoscopic size InAs/GaSb quantum well Hall bar devices in the inverted regime. Using a pair of electrostatic gates we move the Fermi level into the electron-hole hybridization state, observing a mini gap and Van Hove singularity at its edge. Temperature dependence of the conductivity in the gap shows a residual conductivity, which can be consistently explained by the contributions from the free as well as the hybridized carriers in the presence of impurity scattering, as proposed by Naveh and Laikhtman, [Europhys. Lett. **55**, 545 (2001)]. Experimental implications for the stability of proposed quantum spin Hall helical edge states will be discussed.

DOI: 10.1103/PhysRevB.81.201301

PACS number(s): 73.63.Hs, 72.20.-i, 72.25.Dc

It was recently proposed that a novel transport phenomenon, termed the quantum spin Hall effect (QSHE) (Refs. 1–3) should arise in a class of two-dimensional topological insulators (TI). The QSHE phase is characterized by an odd number of Kramer pair states at the edges, and an insulating gap in the bulk. Edge states are robust against disorder due to the topology of the bands and result in helical edge transport. Four-probe transport measurements at zero magnetic field give a near quantized conductance of $2e^2/h$ for mesoscopic samples, as observed in HgTe/CdTe quantum wells.⁴ More recently, Liu *et al.*⁵ proposed to observe QSHE in an inverted InAs/GaSb composite quantum well (CQW), in which the band structure can be tuned with electrical fields,⁶ giving rise to a phase transition from a normal insulator to TI via a continuously varying parameter.

In previous studies of CQW,^{7–10} a mini gap originating from hybridization was observed in capacitance measurements,⁷ and subsequently corroborated in transport studies of double-gated CQW (Ref. 8) and far-infrared measurements.^{9,10} However, a true bulk insulator, with temperature activated conductivity, has yet to be experimentally confirmed. It is crucial to understand the bulk transport since the edge modes are only protected by an insulating gap, and presence of states inside the bulk gap could allow for scattering of edge states between the opposite sides of the sample, destroying helical transport properties.

In CQW, carriers (electrons and holes) are separated in different wells and the bulk energy gap arises due to the hybridization of the e and the h bands at a finite k vector, k_{cross} , in momentum space. This finite k character is in contrast to that in the HgTe QWs, where the carriers are in the same well and the energy gap opens in the zone center. In this Rapid Communication we present an experimental study of low-temperature conductivity in CQW Hall-bar devices. We observed a transport energy gap and the associated Van Hove singularity. Analyses of our results indicate intricate contributions from the free as well as the hybridized carriers to the bulk CQW conductivity in the presence of a finite amount of disorder. Interestingly, such contributions appear to be independent of the amount of scattering but vary strongly with CQW band parameters.¹¹ In particular, shifting

k_{cross} toward zero should reduce the bulk conductivity, thereby promoting the QSHE.

The energy spectrum of CQW is schematically shown in Fig. 1(a). Due to the broken gap alignment of InAs and GaSb, conduction and valence states are confined in InAs and GaSb layers, respectively.¹² For wider wells such as ours, the structure is inverted [Fig. 1(a)], with the ground conduction subband (E1) lower than the ground heavy-hole subband (H1), resulting in anticrossing of the bands at k_{cross} [Fig. 2(a)]. Assuming that band anisotropy is small, anticrossing occurs when carrier densities in two wells are equal, $n=p=k_{cross}^2/2\pi$, corresponding to the resonant condition of equal particle energy and in-plane momentum in two wells. Due to the tunneling-induced coupling, electron and hole states are mixed and a mini-gap Δ opens in otherwise semi-

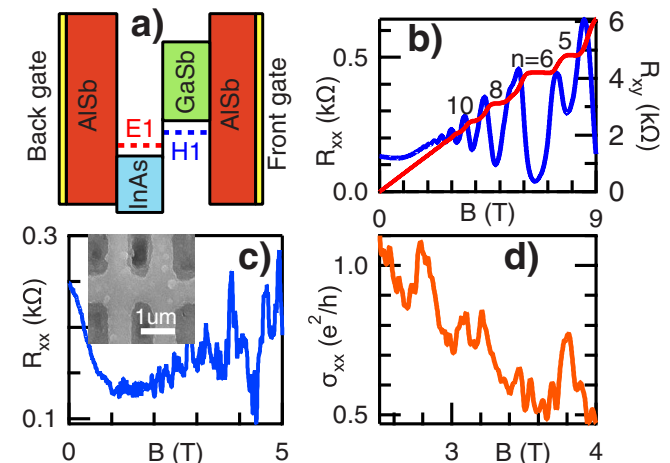


FIG. 1. (Color online) (a) Shows structure and energy spectrum of inverted CQW with $E1 < H1$. Separation of the bands, E_{go} , as well as Fermi energy E_F can be tuned with front and back gates. When $E_F > H1$ are present in the well and representative magnetotransport data at $T=0.3$ K is shown in (b) for $10 \times 20 \mu\text{m}^2$ (sample B) and in (c) for $0.7 \times 1.5 \mu\text{m}^2$ (sample A) Hall bar (scanning electron microscopy image in the inset) where R_{xx} exhibits strong fluctuations. (d) Fluctuations in conductivity (sample A) are on the order of e^2/h , indicating mesoscopic regime.

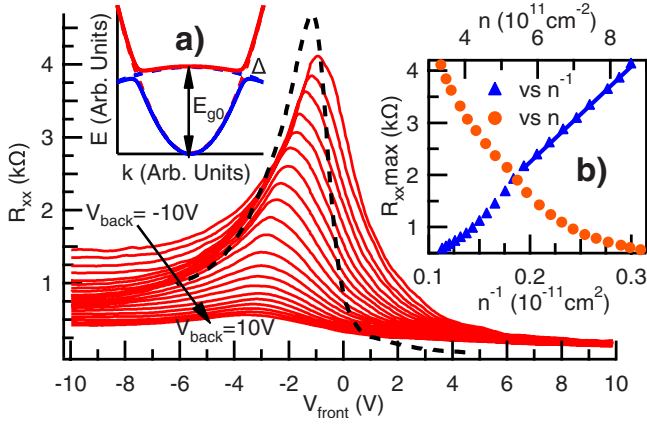


FIG. 2. (Color online) The figure shows R_{xx} vs V_{front} in sample A for V_{back} from 10 to -10 V, in 1 V steps, $B=0$ T, $T=0.3$ K; and in sample B (dashed) for $V_{back}=-10$ V. Inset (a) at the anticrossing point, where $n \sim p$, a hybridization gap Δ opens. For E_F in the gap, R_{xx} exhibits resonance peaks, which decrease for increasing V_{back} . (b) Resonance peaks vary linearly with n^{-1} for $n \leq 5 \times 10^{11}$ cm^{-2} as proposed in Ref. 11.

metallic band dispersion [Fig. 2(a)].⁶ In order to observe the QSHE,⁴ the Hall bar length L should satisfy $L < \lambda_\phi$, where λ_ϕ is the inelastic scattering length and its value is on the order of a few micron in our samples. In large samples ($L \gg \lambda_\phi$), edge mode resistance can be estimated¹³ as $(L/\lambda_\phi)(h/2e^2)$.

Our InAs/GaSb CQW was grown by molecular-beam epitaxy on silicon-doped $\text{N}^+(100)$ GaAs substrate. The structure consists of a standard buffer consisting of AlSb and $\text{Al}_{0.8}\text{Ga}_{0.2}\text{Sb}$ layers.¹⁴ On top of this a 500 Å AlSb lower barrier was grown, followed by 150 Å InAs and 80 Å GaSb quantum wells with a 500 Å AlSb top barrier and a 30 Å GaSb cap layer. Our experiments were performed on two Hall bar samples from the same wafer, processed using standard photo and e-beam lithography with wet etching. The sample A (B) has width and length of 0.7×1.5 μm^2 (10×20 μm^2). The top gate was fabricated by depositing 2500 Å Si_3N_4 using plasma-enhanced chemical vapor deposition system, and evaporating 1000 Å Al or Ti/Au metal gate. N^+GaAs substrate serves as a back gate for our devices and was contacted using silver resin. Ohmic contacts to the electron-hole layers were made with indium and without annealing. Low-temperature magnetotransport measurements were carried out in a ^3He refrigerator (300 mK) combined with a 12 T superconducting magnet, or in a $^3\text{He}/^4\text{He}$ dilution refrigerator (20 mK) with a 18 T magnet (National High Magnetic Field Laboratory, NHMFL). Standard lock-in technique with an excitation current of 100 nA at 23 Hz was employed.

In dual gate geometry [Fig. 1(a)], both the relative separation between the subbands, E_{g0} , and the Fermi energy E_F can be tuned. When E_F is between H1 and E1, electrons and holes coexist in their respective layers, resulting in two-carrier transport⁷ with characteristic nonlinear dependence of Hall resistance, R_{xy} , on magnetic field, B . Single carrier transport occurs for E_F above H1 or below E1, and is electronlike or holelike, respectively. In our CQW, E_F is pinned

by the surface states in the cap layer¹⁵ and under zero applied bias only electrons are present in the well with a typical low-temperature density of 7×10^{11} cm^{-2} and mobility of 90,000 $\text{cm}^2/\text{V s}$. Shubnikov de Haas (SdH) oscillations can be observed starting at 1.8 T with no evidence of parallel conduction. R_{xy} varies linearly with B until the appearance of the integer quantum Hall plateaus. A representative trace for electronlike transport in a larger size Hall bar is shown in Fig. 1(b). In contrast, micron-size devices show strong fluctuations in R_{xx} [Fig. 1(c)]. Fluctuations are reproducible in magnetic field, and conductivity varies on the order of e^2/h [Fig. 1(d)], indicating a mesoscopic regime.

In the single-carrier regime, electron density changes linearly with front and back bias as approximately 1.5×10^{11} cm^{-2}/V and 0.4×10^{11} cm^{-2}/V . Electron densities are extracted by sweeping gate biases at fixed B or through analysis of SdH oscillations. When holes are induced in the GaSb well, the effect of front gate on the electron density in the InAs layer is near-perfectly screened. When induced, holes will coexist with electrons in the device bias range and hole density can be extracted by fitting R_{xy} with two-carrier transport expression. Values are consistent with those for unscreened electrons and in agreement with the parallel capacitor model.

In Fig. 2 we sweep the front bias from 10 to -10 V with the back bias fixed, changing the carriers from solely electrons to predominantly holes, as evidenced from the change in sign in R_{xy} at high B . When the carrier densities are matched (i.e., $n \sim p$), clear peaks in R_{xx} appear, indicating the existence of a mini gap. Resonance peaks, $R_{xx}(\text{max})$, increase with decreasing back bias, and hence vary inversely with resonance electron-hole density, $n=p$ and corresponding k_{cross} (Fig. 2). In particular, for $n \leq 5 \times 10^{11}$ cm^{-2} , resonance peaks vary linearly with n^{-1} [Fig. 2(b)]. This inverse relationship, which we subsequently discuss, cannot be explained with an increasing mini gap, for coupling between wells varies proportionally¹⁶ with k .

Our central finding is the existence of finite conductivity in InAs/GaAs in the mini-gap regime. Even at the lowest temperature $T=20$ mK [Fig. 3(a)], largest observed resonance peaks $R_{xx}(\text{max}) \sim 5$ $\text{k}\Omega$ for mesoscopic samples, which is at least 2–3 times smaller than $h/2e^2$. This is in contrast to the case of HgTe QWs where quantized value is approached from larger resistance values.⁴ Hence, observed resonance peaks can be understood as a bulk effect with a residual conductivity on the order of $10e^2/h$, which is a few times larger than the predicted contribution from the edge. This is corroborated by the fact that sample B (10×20 μm^2) also shows a resistance peak value of ~ 4.5 $\text{k}\Omega$ (shown in Fig. 2, dotted line). We should note that in Ref. 8 a peak resistance value of ~ 15 $\text{k}\Omega$ is reported, which appears close to $h/2e^2$. However, this value presumably reflects only the bulk transport in the macroscopic samples used in Ref. 8, where $L \gg \lambda_\phi$, and is consistent with our measurements if geometric factor is taken into account.

For the remainder of this paper we concentrate on the origin of residual gap conductivity. We first note that the anisotropy of the heavy hole band may play a role in the gap anisotropy at the Fermi energy, which could lead to residual conductivity. Anisotropy is more apparent for larger k_{cross}

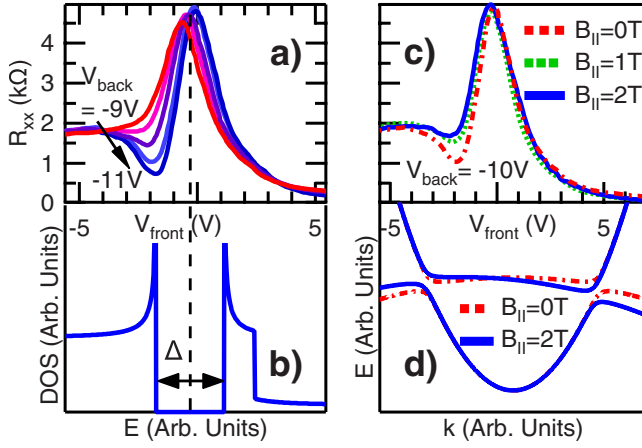


FIG. 3. (Color online) (a) The figure shows R_{xx} vs V_{front} in sample A for V_{back} from -9 to -11 V, in 0.5 V steps, $B=0$ T, $T=20$ mK. Resistance dips occur at singularities in DOS near gap edges shown in (b). From relative position of dips and peaks in V_{front} we determine $\Delta \approx 3.6$ meV. Dips weaken with in-plane magnetic field in (c), due to induced anisotropy in the dispersion in (d).

(Ref. 16) and may explain the decrease in $R_{xx}(\max)$ with larger n (Fig. 2). To what extent such anisotropy would affect the gap value is a subject for numerical calculations with realistic materials parameters.¹⁷

Here we show experimentally that band anisotropy, which may affect the gap, plays a minor role in our transport regime. Measurements at $T=20$ mK reveal clear dips in R_{xx} in the vicinity of resonance peaks, for $V_{back} < -9$ V [Fig. 3(a)].¹⁸ Such regime corresponds to small on-resonance carrier densities, and observed dips can be explained by Van Hove singularities in density of states (DOS) [Fig. 3(b)] at gap edges.¹⁶ The fact that such singularities have been observed in transport attests to the high quality of our samples. Resistance dips occur only for smaller k due to otherwise increasing anisotropy of the valence band, smearing out DOS singularities. Applying in-plane magnetic field [Fig. 3(d)] induces anisotropy in the direction of the field⁷ and dips weaken [Fig. 3(c)]. Width of the singularity is thus $\Delta k = eB_{||}\langle z \rangle / \hbar = 0.035$ nm⁻¹, where $\langle z \rangle$ is one-half thickness of CQW (Ref. 7) and corresponding anisotropy in energy is $\Delta E \approx k \cdot \Delta k / \pi \text{DOS} = 0.9$ meV, where $k = 0.14$ nm⁻¹ and $\text{DOS} = (m_e + m_h) / \pi \hbar^2$, with carrier masses $m_e = 0.03$ and $m_h = 0.37$ (in units of free-electron mass).⁷ Thus, at least in the small carrier-density regime band anisotropy cannot be responsible for the observed residual conductivity. We note that resistance dips are observed only on the hole side of the mini gap, which could be attributed to the smaller E_{g0} , i.e., smaller k , which decreases for more negative V_{front} , as well as a strong M shape of the valence band.⁶

We estimate the gap value from the relative position of resistance dips and peaks [Figs. 3(a) and 3(b)] in front gate bias as: $\Delta = 2(V_{peak} - V_{dip}) \frac{\Delta p}{\Delta V} \frac{1}{\text{DOS}}$, where $\frac{\Delta p}{\Delta V}$ is the rate of carrier-density change with front bias. We obtain $\Delta = 3.6$ meV, in agreement with previous studies.^{7,8,10} Similar value can be deduced from temperature dependence of resonance peaks [Fig. 4(a)], which shows insulating character, i.e., $R_{xx}(\max)$ increases in lowering T . On the other hand, we

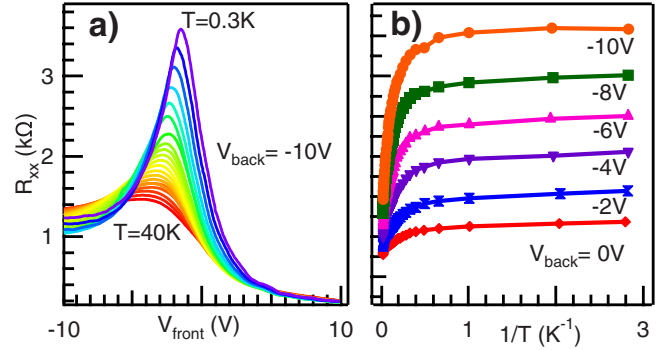


FIG. 4. (Color online) (a) The figure shows temperature dependence of resonance peaks in sample A for $V_{back} = -10$ V for T from 0.3 to 40 K consecutively in roughly 2 K steps. (b) Resonance peaks shown vs T^{-1} saturate for $T < 2$ K, for six different k_{cross} .

do not observe temperature-activated resistance, as one would expect for a true insulator. Resonance peaks increase only by a factor of $2-3$ over three orders of magnitude change in temperature, for six anticrossing points measured, and saturate for $T < 2$ K [Fig. 4(b)]. Nevertheless, peaks persist up to 40 K for all six cases, consistent with a gap value of $3-4$ meV.

For further analysis we determine the carrier scattering times characterizing the transport in a zero magnetic field. At zero bias, electron scattering time is $\tau_r = 1.5$ ps and the associated level broadening is $\Gamma_e = \hbar / 2\tau_r = 0.2$ meV. Electron mobility shows linear dependence on electron density and drops to approximately $40,000$ cm²/V s for the case of smallest electron density of 3.3×10^{11} cm⁻², giving $\Gamma_e = 0.5$ meV. Linear dependence of mobility on electron density is indicative of short-range scattering, presumably from dislocations at interfaces, which is confirmed by extracting the quantum time τ_q from SdH oscillations,¹⁹ giving $\tau_r / \tau_q \approx 7$ at zero bias and validating predominance of large angle scattering. Estimated τ_q has been corrected for density inhomogeneity²⁰ with Gaussian width of $\delta n \approx 0.35 \times 10^{11}$ cm⁻². On a side note, this suggests that the random potential fluctuations are on the order of $\delta E = \delta n / \text{DOS} \sim 0.25$ meV, and thus $\delta E \ll \Delta$. For holes, $\Gamma_h = b \frac{m_e}{m_h} \Gamma_e$, where b is the ratio of electron to hole mobilities. From a fit to R_{xy} in two-carrier transport regime, $b \approx 6$, giving $\Gamma_h = 0.3$ meV. Thus, total level broadening is less than $\Gamma = \Gamma_e + \Gamma_h \approx 0.8$ meV, which is a few times smaller than the size of the gap, indicating that disorder may play only nontrivial role.

Naveh and Laikhtman¹¹ have theoretically studied the transport in the inverted regime of InAs/GaAs system, concluding that even negligible but finite-level broadening due to the carrier scattering will result in finite on-resonance conductivity at $T=0$ K. Specifically, residual conductivity will go as $\sigma_{on}(T=0) \sim \frac{e^2 E_{g0}}{h \Delta}$, when $\Gamma \ll \Delta \ll E_{g0}$, thus independent of scattering parameters. Since $E_{g0} = n \frac{\pi \hbar^2}{m^*}$, where $m^* = \frac{m_e m_h}{m_e + m_h}$, it follows that $R_{xx}(\max) \sim n^{-1}$ as observed in Fig. 2(b) for $n \leq 5 \times 10^{11}$ cm⁻². In addition, using result from Ref. 11 and smallest resonance density $n = 3.3 \times 10^{11}$ cm⁻² gives $\sigma_{on} \sim 7 \frac{e^2}{h}$, consistent with our measurements.

Such result can be understood by re-examining the origi-

nal premise for carrier hybridization, which is the nonlocality of electron states in growth direction of the wells.²¹ This nonlocality can be suppressed through carrier scattering, destroying carrier hybridization. The relevant time scale is carrier tunneling time, $\tau_t = \hbar/2\Delta$, and in the relaxation-time model, the total number of scattered carriers within τ_t will go as $n \cdot (1 - e^{-\tau_t/\tau_r})$, or equivalently as $n \cdot (1 - e^{-\Gamma/\Delta})$. Ignoring smaller contribution from scattered holes and using $\mu_e = \frac{e}{m} \frac{\hbar}{2\Gamma}$, we obtain $\sigma_{on} \sim \frac{e^2 E_{g0}}{h \Gamma} (1 - e^{-\Gamma/\Delta})$, recovering $\sigma_{on} \sim \frac{e^2 E_{g0}}{h \Delta}$ for $\Gamma \ll \Delta$. Furthermore, even hybridized states will contribute to residual conductivity, σ_{on} , due to level-broadening-induced charge of hybridized states. In a two-band calculation,²² expectation value of this charge goes as $e \cdot \Gamma/\Delta$ for $\Gamma \ll \Delta$, and since $\mu \propto 1/\Gamma$, this produces additional contribution to σ_{on} also on the order of $\frac{e^2 E_{g0}}{h \Delta}$.

In conclusion, our experiment confirmed the existence of a hybridization-induced energy gap in inverted InAs/GaSb. However, we observed a finite bulk conductivity in the gap regime, which can be reasonably explained by the model proposed in Ref. 11. It would be interesting to investigate

systematically the transport in CQWs having different band parameters especially a reduced E_{g0} , which might lead to a diminishing bulk conductivity in the gap. In particular, a viable regime for QSHE could exist near the critical point, where the band structure changes from inverted to normal. Our work in this parameter regime is in progress.

We gratefully acknowledge S.-C. Zhang and D. C. Tsui for bringing our attention to QSHE in InAs/GaSb system, H. Kroemer for invaluable advices on materials, J. Kono, X.-L. Qi, and Kai Chang for very helpful discussions. We thank A. Ikhlassi for the MBE growth of wafers. The work at Rice was supported by Welch Foundation under Grant No. C-1682, and a Rice Faculty Initiative Fund. Travel to NHMFL was supported by NSF under Grant No. DMR-0706634. A portion of this work was performed at the National High Magnetic Field Laboratory, which is supported by NSF Cooperative under Agreement No. DMR-0084173, by the State of Florida, and by the DOE. We thank T. P. Murphy and J. H. Park for expert technical assistance.

*ik5@rice.edu

¹C. L. Kane and E. J. Mele, *Phys. Rev. Lett.* **95**, 226801 (2005).

²B. A. Bernevig and S. C. Zhang, *Phys. Rev. Lett.* **96**, 106802 (2006).

³B. A. Bernevig, T. L. Hughes, and S.-C. Zhang, *Science* **314**, 1757 (2006).

⁴M. Konig, S. Wiedmann, C. Brune, A. Roth, H. Buhmann, L. W. Molenkamp, X.-L. Qi, and S.-C. Zhang, *Science* **318**, 766 (2007).

⁵C. Liu, T. L. Hughes, X.-L. Qi, K. Wang, and S.-C. Zhang, *Phys. Rev. Lett.* **100**, 236601 (2008).

⁶Y. Naveh and B. Laikhtman, *Appl. Phys. Lett.* **66**, 1980 (1995).

⁷M. J. Yang, C. H. Yang, B. R. Bennett, and B. V. Shanabrook, *Phys. Rev. Lett.* **78**, 4613 (1997).

⁸L. J. Cooper, N. K. Patel, V. Drouot, E. H. Linfield, D. A. Ritchie, and M. Pepper, *Phys. Rev. B* **57**, 11915 (1998).

⁹J. Kono, B. D. McCombe, J. P. Cheng, I. Lo, W. C. Mitchel, and C. E. Stutz, *Phys. Rev. B* **55**, 1617 (1997).

¹⁰M. J. Yang, C. H. Yang, and B. R. Bennett, *Phys. Rev. B* **60**, R13958 (1999).

¹¹Y. Naveh and B. Laikhtman, *Europhys. Lett.* **55**, 545 (2001).

¹²H. Kroemer, *Physica E* **20**, 196 (2004).

¹³See, e.g., S. Datta, *Electronic Transport in Mesoscopic Systems* (Cambridge University Press, Cambridge, 1995).

¹⁴C. Nguyen, B. Brar, C. R. Bolognesi, J. J. Pekarik, H. Kroemer, and J. H. English, *J. Electron. Mater.* **22**, 255 (1993).

¹⁵C. Nguyen, B. Brar, H. Kroemer, and J. H. English, *Appl. Phys. Lett.* **60**, 1854 (1992).

¹⁶S. de-Leon, L. D. Shvartsman, and B. Laikhtman, *Phys. Rev. B* **60**, 1861 (1999).

¹⁷J. Li, W. Yang, and K. Chang, *Phys. Rev. B* **80**, 035303 (2009).

¹⁸In dilution refrigerator carrier densities are (10–15)% lower than in the ³He system due to different sample cooling process. Low-density regime, which shows resistance dips, was not accessible in the ³He system.

¹⁹P. T. Coleridge, *Phys. Rev. B* **44**, 3793 (1991).

²⁰S. Syed, M. J. Manfra, Y. J. Wang, R. J. Molnar, and H. L. Stormer, *Appl. Phys. Lett.* **84**, 1507 (2004).

²¹A. Palevski, F. Beltram, F. Capasso, L. Pfeiffer, and K. W. West, *Phys. Rev. Lett.* **65**, 1929 (1990).

²²G. R. Aizin, B. Laikhtman, and G. Gumbs, *Phys. Rev. B* **64**, 125317 (2001).